HEP-IFUAP-02-03
OITS-729
SHEP-03-05

The di-photon signature of Higgs bosons in GMSB models at the LHC

J. Lorenzo Diaz-Cruz[a1], Dilip Kumar Ghosh[b2] and Stefano Moretti[c3]

[a] *Instituto de Fisica, BUAP, Puebla 72570, Mexico*

[b] *Institute of Theoretical Science, University of Oregon, Eugene OR 97403-5203, USA*

[c] *Department of Physics & Astronomy, University of Southampton, Highfield, Southampton SO17 1BJ, UK*

Abstract

We show how the well studied $\gamma\gamma$ inclusive Higgs signal can be used at the Large Hadron Collider to test Gauge Mediated Supersymmetry Breaking scenarios in which a rather heavy Higgs boson decays into two light neutralinos, the latter yielding two photons and missing (transverse) energy.

PACS Nos.: 13.85.-t, 12.60.Fr, 12.60.Jv, 14.70.Bh

[1]ldiaz@sirio.ifuap.buap.mx

[2]dghosh@physics.uoregon.edu

[3]stefano@hep.phys.soton.ac.uk

1 Introduction

The $\gamma\gamma$ (or 'di-photon') inclusive signature is possibly the most studied one experimentally, in the context of the Large Hadron Collider (LHC), since it allows for the detection of a relatively light ($\lesssim 130$ GeV) neutral Higgs boson, both within the Standard Model (SM) and the Minimal Supersymmetric Standard Model (MSSM) [1, 2]. In fact, the existence of such a light particle state has been hinted already by LEP2 data, both as a possible resonance in the region $M_{\rm Higgs} \approx 115$ GeV and as the mass range that best accommodates the higher order Higgs boson contributions to precision Electroweak (EW) data (see, e.g., [3], for a review).

Despite having a Branching Ratio (BR) that is only at the permille level, the di-photon signature is preferred to the one associated with the main Higgs decay channel in the above mass region, i.e., Higgs $\to b\bar{b}$ (into pair of b-quark jets, with BR practically one), as the latter is swamped by the huge QCD background typical of a hadronic machine, whereas the former is much cleaner in such an environment. Besides, the higher precision that one can achieve in determining both directions and energies of the photons (as compared to those of jets), allows one to obtain a Higgs mass resolution of the order 2–3 GeV, which compares rather well to a typical 15–20 GeV accuracy from jet events, also recalling that the Higgs width is at most a few tens of MeV in the above mass region (so that, the worse the mass resolution the larger the background, while the signal size remains relatively stable) [4].

The di-photon signature may also represent a distinctive signature of broken Supersymmetry (SUSY), namely, in Gauge Mediated Supersymmetry Breaking (GMSB) models [5]. In these scenarios, the Lightest SUSY Particle (LSP) is the so-called gravitino, $\widetilde{G}$. Moreover, the next-to-LSPs (NLSPs) are usually the lightest neutralino, $\widetilde{\chi}_1^0$, or the lighter stau, $\widetilde{t}_1$, depending upon the actual configuration of the GMSB model. In the first case then, the following decay chain could well occur: Higgs $\to \widetilde{\chi}_i^0\widetilde{\chi}_j^0 \to \gamma\gamma \ + \ E_{\rm miss}$ $(i,j=1,2)$, where the missing (transverse) energy is due to the two LSPs and possibly neutrinos (from $\widetilde{\chi}_2^0 \to \widetilde{\chi}_1^0 + \nu\bar{\nu}$) escaping detection[4].

Current collider limits however forbid the lightest MSSM Higgs boson, h, to decay into two neutralinos, i.e., $M_h < M_{\widetilde{\chi}_i^0} + M_{\widetilde{\chi}_j^0}$ $(i,j=1,2)$, so that only the two heavier neutral Higgs bosons, H, A, can initiate the above SUSY decay chain. Recalling that $h \to \gamma\gamma$ direct decays can still occur in GMSB models, it is intriguing to consider the possibility that *all* neutral Higgs bosons of the MSSM can be detected in the same channel, that is, a pair of photons accompanied by

[4]Notice that, within the MSSM, one can obtain the di-photon signature (including $E_{\rm miss}$) of heavy Higgs bosons also from non-GMSB scenarios in which the LSP is the lightest neutralino, $\widetilde{\chi}_1^0$, such as in (minimal) Supergravity (mSUGRA) models. In fact, the following decay chain can occur here: $H/A \to \widetilde{\chi}_2^0\widetilde{\chi}_2^0$ followed by a double radiative decay $\widetilde{\chi}_2^0 \to \widetilde{\chi}_1^0\gamma$ [6]. It has been shown in Ref. [7] that this channel can be large if $\tan\beta$ (see below for its definition) is small ($\simeq 1$), with or without gaugino mass unification at high scales. However, this MSSM configuration is ruled out by the LEP2 limit on the lighter chargino mass [8]. Only under the assumption of non-universal gaugino masses can the BR($\widetilde{\chi}_2^0 \to \widetilde{\chi}_1^0\gamma$) be large at high $\tan\beta$ in mSUGRA models [9].

some amount of missing (transverse) energy, $E_{\rm miss}$. Notice that the latter should in average be larger for signal events as compared to the background, which is dominated by prompt di-photon production, where $E_{\rm miss}$ is mainly due to jet energy losses down the beam pipe or to non-fully hermetic detectors. In contrast, one would naturally expect a large $E_{\rm miss}$ value arising from the above H and A decays (if not from invisible decay products of heavy particles produced in association with any of the Higgs states, see below), so that the missing (transverse) energy may be used in the kinematical selection. In practice though, only two resonances could in the end be visible, as the H and A bosons are almost degenerate in mass. Besides, the latter would tend to be located at higher $\gamma\gamma$ invariant masses as compared to the one due to $h \to \gamma\gamma$ decays, where the production cross section is smaller, but so is the di-photon continuum.

Finally, whereas the $h \to \gamma\gamma$ resonance can directly be reconstructed from the photon four-momenta, the same is not true in the $H, A \to \widetilde{\chi}_i^0 \widetilde{\chi}_j^0 \to \gamma\gamma \ + \ E_{\rm miss}$ $(i, j = 1, 2)$ channel. Here, however, after ensuring that the two photons are not back-to-back, one can attempt to resolve the $E_{\rm miss}$ along their directions and add it to the photonic transverse momenta, $p_T^{\gamma_1}$ and $p_T^{\gamma_2}$. Scaling up the respective sums by the ratios $p^{\gamma_1}/p_T^{\gamma_1}$ and $p^{\gamma_2}/p_T^{\gamma_2}$ gives in principle the reconstructed momenta of the neutralino pair. In practice though, the presence of several unresolved sources of missing (transverse) energy may spoil the mass reconstruction.

It is the purpose of this paper to investigate in detail such a phenomenology, in the context of GMSB scenarios. After a brief discussion of the parameters defining GMSB models and a description of the tools used in order to carry out our numerical studies, we will present the results and draw our conclusions.

2 The spectrum in GMSB models

In GMSB models, the symmetry of the Superpotential is broken at some relatively low scale, say, a few hundred TeV (the 'hidden sector'), and SUSY-breaking is communicated to the detectable particles (the 'visible sector') through so-called 'messenger' fields, effectively, gauge bosons.

In fact, renormalisability of the theory, coupled with economy of field content, dictates that the messenger sector (MS) be comprised of chiral Superfields such that their SM gauge couplings are vectorial in nature. Most GMSB models actually consider these fields to be in $(5+\bar{5})$ or $(10+\overline{10})$ representations of SU(5). They are also chosen to transform as a multiplet of a Grand Unification Theory (GUT), so that the SUSY prediction of gauge coupling unification is preserved. These facts restrict the maximum number of messenger families N_M to be ≤ 4 and ≤ 1 for the $(5+\bar{5})$ and $(10+\bar{1}0)$ constructs, respectively.

Limiting ourselves, for the time being, to a single pair of MS Supermultiplets $(\Psi+\bar{\Psi})$, consider a term in the Superpotential of the form $\lambda \mathcal{S} \bar{\Psi} \Psi$, where $\mathcal{S}$ is a SM singlet. The scalar (S) and auxiliary (F_S) components of $\mathcal{S}$ may acquire Vacuum Expectation Values (VEVs) through their

interactions with the hidden sector fields. SUSY-breaking is thus communicated to the MS, with the fermions and sfermions acquiring different masses. This, in turn, is communicated to the SM fields resulting in the gauginos and sfermions acquiring masses at the one-loop and two-loop levels, respectively. The expressions, in the general case of multiple messenger pairs and/or gauge singlets $\mathcal{S}_i$, is a somewhat complicated function [5] of $M \equiv \langle S \rangle$ and $\Lambda \equiv \langle F_S \rangle / \langle S \rangle$. However, if there is just one such singlet, the expressions for soft SUSY-breaking gaugino and scalar masses at the messenger scale M simplify to:

$$\tilde{M}_i(M) = N_M \frac{\alpha_i(M)}{4\pi} g_1\left(\frac{\Lambda}{M}\right)\Lambda, \tag{1}$$

$$\tilde{m}^2_{\tilde{f}}(M) = 2N_M\Lambda^2 g_2\left(\frac{\Lambda}{M}\right)\sum_{i=1}^{3}\kappa_i C_i^{\tilde{f}}\left(\frac{\alpha_i(M)}{4\pi}\right)^2. \tag{2}$$

In eq. (2), $C_i^{\tilde{f}}$ are the quadratic Casimirs for the sfermion in question. The factors κ_i equal 1, 1 and 5/3 for SU(3), SU(2) and U(1), respectively, with the gauge couplings so normalised that all $\kappa_i\alpha_i$'s are equal at the messenger scale. The threshold functions are given by

$$g_1(x) = \frac{1+x}{x^2}\log(1+x) + (x \to -x), \tag{3}$$

$$g_2(x) = \frac{(1+x)}{x^2}\left[\log(1+x) + 2\mathrm{Li}_2\left(\frac{x}{1+x}\right) - \frac{1}{2}\mathrm{Li}_2\left(\frac{2x}{1+x}\right)\right] + (x \to -x). \tag{4}$$

The Superparticle masses at the EW scale are obtained from those in eqs. (1)–(2) by evolving the appropriate Renormalisation Group Equations (RGEs). For the scalar masses, the D-terms need to be added too. The Higgs sector of the 'minimal' GMSB model contains the two usual Higgs doublets of the MSSM, (H_u, H_d). The ratio of the VEVs of the latter is parameterised as $\tan\beta = \frac{v_u}{v_d}$. Moreover, in the Superpotential one has a Higgs bilinear term of the form $B\mu H_u H_d$. In general, μ and B depend on the details of the SUSY-breaking mechanism. However, if we assume that the EW symmetry is broken radiatively, then the values of μ^2 and B are determined in terms of the other parameters of the model. Without loss of generality, one may express the entire particle spectrum of such a GMSB model in terms of five external inputs only: $M, \Lambda, \tan\beta$, $\mathrm{sgn}(\mu)$ and N_M (hereafter, we assume $N_M = 1$).

3 Parameter scans

As a starting point of our investigation, we shall discuss the relevant particle spectrum by searching for regions of the GMSB parameter space where the heavy Higgs bosons, H and A, and the lightest neutralino, $\widetilde{\chi}_1^0$, have masses and compositions (in terms of the gaugino-Higgsino fields) such that the decays $H, A \to \widetilde{\chi}_1^0\widetilde{\chi}_1^0$ are kinematically allowed and reach BRs that are at least comparable to that of the SM Higgs decay into two photons, for which one has $\mathrm{BR}(H_{\mathrm{SM}} \to \gamma\gamma) \simeq 10^{-3}$. In fact, such a channel is of extreme importance in the MSSM too, as already noted. Here, the

parameters $\tan\beta$ and M_A define entirely the Higgs sector of the MSSM at tree-level, $\tan\beta$ having being already defined and with M_A being the mass of the pseudoscalar Higgs state A (the other two states, h and H, are scalars)[5]. It turns out that, for any $\tan\beta$ value, if $M_A \gtrsim 150$–200 GeV, the $h \to \gamma\gamma$ decay mode is a discovery channel of the lightest Higgs boson of the MSSM.

In order to sample the strength of the di-photon signal of our interest, we present a set of numerical results that include the Higgs and lightest neutralino masses, as well as the BRs of the channels $H, A \to \widetilde{\chi}_1^0\widetilde{\chi}_1^0$. In computing these rates we have used the subroutines of ISAJET 7.58 [10] that implement the GMSB model, with several choices of parameter inputs. Namely, in Tabs. 1,2 and 3 we have fixed $M = 150$ TeV and taken $\Lambda = 75, 100$ and 125 TeV, respectively. Here, the sign of μ is always negative whereas $\tan\beta$ varies from 5 up to a maximum value where the decays $H, A \to \widetilde{\chi}_1^0\widetilde{\chi}_1^0$ are no longer kinematically allowed.

From Tabs. 1–3 one can appreciate the following trends.

- As intimated in the Introduction, the Higgs masses M_H and M_A show a degeneracy within a couple of GeVs. Thus, we can add their corresponding two-photon signals, as it would not be possible to distinguish among them solely on the basis of the reconstructed mass.

- The lightest neutralino $\widetilde{\chi}_1^0$ decays into a photon plus a gravitino, $\widetilde{\chi}_1^0 \to \gamma + \widetilde{G}$, while $\mathrm{BR}(H, A \to \widetilde{\chi}_1^0\widetilde{\chi}_1^0)$ can exceed the 10^{-3} level, this yielding altogether a decay rate for the channels $H, A \to \widetilde{\chi}_1^0\widetilde{\chi}_1^0 \to \gamma\gamma + E_{\rm miss}$ above our reference di-photon SM Higgs decay rate.

- For values of $\tan\beta$ larger than 40 or so, the decays $H, A \to \widetilde{\chi}_1^0\widetilde{\chi}_1^0$ are no longer kinematically allowed.

Table 1: Higgs, lightest neutralino masses and $\mathrm{BR}(H, A \to \widetilde{\chi}_1^0\widetilde{\chi}_1^0)$ for a sample set of GMSB inputs with $(M, \Lambda) = (150, 75)$ TeV.

$\tan\beta$	M_H [GeV]	M_A [GeV]	$M_{\widetilde{\chi}_1^0}$ [GeV]	BR(H)	BR(A)
5	430	428	105	1.4×10^{-2}	1.1×10^{-2}
10	404	403	104	1.1×10^{-2}	1.2×10^{-2}
15	392	391	103	6.0×10^{-3}	7.3×10^{-3}
20	377	377	103	3.5×10^{-3}	4.6×10^{-3}
25	358	358	103	2.1×10^{-3}	3.0×10^{-3}
30	332	332	103	1.3×10^{-3}	2.0×10^{-3}
35	296	296	103	7.5×10^{-4}	1.4×10^{-3}
40	245	245	102	2.5×10^{-4}	7.9×10^{-4}
45	162	161	102	0	0

[5]In fact, in the GMSB model, all Higgs masses are derived quantities, as specified in the previous Section.

Table 2: Higgs, lightest neutralino masses and BR($H, A \to \widetilde{\chi}_1^0\widetilde{\chi}_1^0$) for a sample set of GMSB inputs with $(M, \Lambda) = (150, 100)$ TeV.

$\tan\beta$	M_H [GeV]	M_A [GeV]	$M_{\widetilde{\chi}_1^0}$ [GeV]	BR(H)	BR(A)
5	552	551	146	7.6×10^{-3}	7.5×10^{-3}
10	521	520	145	7.1×10^{-3}	8.6×10^{-3}
15	505	505	145	3.7×10^{-3}	4.9×10^{-3}
20	488	487	144	2.1×10^{-3}	3.0×10^{-3}
25	464	464	144	1.2×10^{-3}	1.9×10^{-3}
30	433	432	144	7.6×10^{-4}	1.3×10^{-3}
35	390	389	144	4.1×10^{-4}	8.6×10^{-4}
40	330	330	144	1.2×10^{-4}	4.7×10^{-4}
45	237	237	144	0	0

Table 3: Higgs, lightest neutralino masses and BR($H, A \to \widetilde{\chi}_1^0\widetilde{\chi}_1^0$) for a sample set of GMSB inputs with $(M, \Lambda) = (150, 125)$ TeV.

$\tan\beta$	M_H [GeV]	M_A [GeV]	$M_{\widetilde{\chi}_1^0}$ [GeV]	BR(H)	BR(A)
5	666	664	197	4.8×10^{-3}	5.4×10^{-3}
10	628	628	195	4.8×10^{-3}	6.5×10^{-3}
15	610	610	195	2.5×10^{-3}	3.7×10^{-3}
20	590	589	195	1.4×10^{-3}	2.2×10^{-3}
25	562	562	195	7.9×10^{-4}	1.4×10^{-3}
30	526	526	195	4.4×10^{-4}	9.3×10^{-4}
35	477	476	195	2.1×10^{-4}	5.9×10^{-4}
40	408	408	194	2.3×10^{-5}	2.3×10^{-4}
45	306	305	194	0	0

For some regions of the GMSB parameter space, the decays $H, A \to \widetilde{\chi}_1^0\widetilde{\chi}_2^0, \widetilde{\chi}_2^0\widetilde{\chi}_2^0$, followed by $\widetilde{\chi}_2^0 \to \widetilde{\chi}_1^0 + X$ can be significant enough to contribute to the two-photon signals. Although this effect was not included in the previous Tables, as it was small, it will be considered in the remainder of this Section and in the Monte Carlo (MC) simulations of the next one as well. To discuss their effects, we have produced three additional sample points, which we elaborate upon below and in Tabs. 4–6, before moving on to the event generator analysis.

Tab. 4 corresponds to the Snowmass slope $M = 2\Lambda$ [11], as we have fixed $\tan\beta = 15$ and taken sgn(μ) positive, further varying Λ from 75 to 150 TeV (for lower values of Λ we get a chargino lighter than 150 GeV, which is not allowed by current collider bounds [12]). Both the

BR columns (BR(H) and BR(A)) contain three rows, each corresponding from top to bottom to the decay rates of H and A into $\widetilde{\chi}_1^0\widetilde{\chi}_1^0$, $\widetilde{\chi}_1^0\widetilde{\chi}_2^0$ and $\widetilde{\chi}_2^0\widetilde{\chi}_2^0$ pairs, respectively.

For these sets of GMSB parameter space points the BR of H and A into $\widetilde{\chi}_1^0\widetilde{\chi}_2^0$ always dominates over the other two channels. This can be understood in terms of the enhancement of the $H, A - \widetilde{\chi}_1^0 - \widetilde{\chi}_2^0$ coupling, which over-compensates the phase-space suppression in the $H, A \to \widetilde{\chi}_1^0\widetilde{\chi}_2^0$ decay modes. Furthermore, one can see from Tab. 4 that, as Λ increases, the Higgs masses M_H and M_A become rather heavy and they still show degeneracy. The discussed BRs stay above 10^{-3}, but because the production rate decreases substantially for Higgs masses above about 600 GeV, only the lower values of Λ ($\simeq 75$ TeV) will produce sizable signals. It is interesting to note that in this case the BR of the lightest Higgs boson into two photons remains close to the SM value, with $M_h \simeq 115$ GeV.

Table 4: Higgs, lightest and second lightest neutralino masses and BR($H, A \to \widetilde{\chi}_1^0\widetilde{\chi}_1^0, \widetilde{\chi}_1^0\widetilde{\chi}_2^0, \widetilde{\chi}_2^0\widetilde{\chi}_2^0$) for a sample set of GMSB inputs with $M = 2\Lambda$, $\tan\beta = 15$ and sgn(μ) positive.

Λ [TeV]	M_H [GeV]	M_A [GeV]	$M_{\widetilde{\chi}_1^0}$ [GeV]	$M_{\widetilde{\chi}_2^0}$ [GeV]	BR(H)	BR(A)
75	395	394	101	184	7.5×10^{-3}	1.0×10^{-2}
					2.08×10^{-2}	4.4×10^{-2}
					4.01×10^{-3}	3.3×10^{-2}
80	419	418	108	198	6.5×10^{-3}	9.3×10^{-3}
					1.8×10^{-2}	4.1×10^{-2}
					3.05×10^{-3}	3.02×10^{-2}
90	467	466	123	225	5.2×10^{-3}	7.6×10^{-3}
					1.56×10^{-2}	3.7×10^{-2}
					1.56×10^{-3}	2.4×10^{-2}
100	515	514	137	252	4.2×10^{-3}	6.2×10^{-3}
					1.32×10^{-2}	3.25×10^{-2}
					6.47×10^{-4}	1.74×10^{-2}
125	631	631	173	320	2.8×10^{-3}	4.3×10^{-3}
					9.2×10^{-3}	2.55×10^{-2}
					-	-
150	745	744	209	387	2.0×10^{-3}	3.2×10^{-3}
					6.9×10^{-3}	2.1×10^{-2}
					-	-

Table 5: Higgs, lightest and second lightest neutralino masses and BR($H, A \to \widetilde{\chi}_1^0\widetilde{\chi}_1^0, \widetilde{\chi}_1^0\widetilde{\chi}_2^0, \widetilde{\chi}_2^0\widetilde{\chi}_2^0$) for a sample set of GMSB inputs with $M = 2\Lambda$, $\Lambda = 75$ TeV, $\tan\beta = 10$ and sgn(μ) positive.

Λ [TeV]	M_H [GeV]	M_A [GeV]	$M_{\widetilde{\chi}_1^0}$ [GeV]	$M_{\widetilde{\chi}_2^0}$ [GeV]	BR(H)	BR(A)
75	405	404	101	183	1.54×10^{-2} 4.36×10^{-2} 1.2×10^{-2}	2.0×10^{-2} 8.5×10^{-2} 7.0×10^{-2}

Table 6: Higgs, lightest and second lightest neutralino masses and BR($H, A \to \widetilde{\chi}_1^0\widetilde{\chi}_1^0, \widetilde{\chi}_1^0\widetilde{\chi}_2^0, \widetilde{\chi}_2^0\widetilde{\chi}_2^0$) for a sample set of GMSB inputs with $M = 2\Lambda$, $\Lambda = 75$ TeV, $\tan\beta = 35$ and sgn(μ) negative.

Λ [TeV]	M_H [GeV]	M_A [GeV]	$M_{\widetilde{\chi}_1^0}$ [GeV]	$M_{\widetilde{\chi}_2^0}$ [GeV]	BR(H)	BR(A)
75	296	296	102	188	7.53×10^{-4} 9.73×10^{-5} -	1.4×10^{-3} 2.0×10^{-3} -

4 Monte Carlo simulation of signal and background

In this section, we evaluate the inclusive production cross sections at the LHC for the two heavy neutral Higgs bosons of the MSSM, H and A, each followed by all possible decays yielding two photons and missing (transverse) energy.

Hereafter, we make the assumption that coloured SUSY particles (chiefly, squarks) are heavy enough[6] so that they do not enter the loops in the '$gg \to$ Higgs' production mode nor they can produce Higgs bosons in cascade decays or enter the Higgs decay chains (the same for gluinos). Alongside the mentioned gluon-fusion channel, we consider the following Higgs production modes: '$q\bar{q}, gg \to Q\bar{Q}$ Higgs' (associated heavy-quark production), '$qq \to qqV^*V^* \to qq$ Higgs' (vector-fusion) and '$q\bar{q}^{(\prime)} \to V$ Higgs' (Higgs-strahlung), with q representing all possible combinations of light (anti)quarks and where $Q = b, t$, $V = W^{\pm}, Z$ and Higgs $= H, A$ (except in the last two modes, where the pseudoscalar Higgs boson cannot be produced). These are the leading production modes of neutral Higgs states of the MSSM at the LHC (under the above assumption of heavy squarks and gluinos)[7] and have been computed here at next-to-leading order accuracy, by adopting the programs described at [14], with default settings.

As for the calculation of the SUSY decays rates (again, produced with ISAJET v7.58), we have adopted the GMSB configurations given in Tab. 7 for M and Λ, further varying $\tan\beta$ from 5 to 40, always with sgn(μ) > 0. (Note that all the above choices of SUSY parameters are allowed by the lighter chargino mass limit, as derived within the GMSB model.)

[6] As it is typical in most GMSB scenarios.

[7] See Ref. [13] for a review of their properties.

Table 7: Sets of GMSB parameter points M and Λ considered in Fig. 1.

Point	M [TeV]	Λ [TeV]
A	150	75
B	150	100
C	150	125
D	200	75
E	200	100
F	200	125
G	200	150
H	200	175

We define the 'effective' production rate of the $\gamma\gamma + E_{\rm miss}$ signature, $\sigma_{\rm eff}$, as:

$$\begin{aligned}
\sigma_{\rm eff} &= \sigma(gg \to H) \times {\rm BR}_{\rm eff}(H) \\
&+ \sigma(gg \to A) \times {\rm BR}_{\rm eff}(A) \\
&+ \sigma(q\bar{q}, gg \to Q\bar{Q}H) \times {\rm BR}_{\rm eff}(H) \\
&+ \sigma(q\bar{q}, gg \to Q\bar{Q}A) \times {\rm BR}_{\rm eff}(A) \\
&+ \sigma(q\bar{q} \to HV) \times {\rm BR}_{\rm eff}(H) \\
&+ \sigma(qq \to qqH) \times {\rm BR}_{\rm eff}(H) \qquad (5)
\end{aligned}$$

where ${\rm BR}_{\rm eff}(H)$ and ${\rm BR}_{\rm eff}(A)$ are defined as follows:

$$\begin{aligned}
{\rm BR}_{\rm eff}(H/A) &= \Bigg[{\rm BR}\Big(H/A \to \widetilde{\chi}_1^0\widetilde{\chi}_1^0\Big) + {\rm BR}\Big(H/A \to \widetilde{\chi}_1^0\widetilde{\chi}_2^0\Big) \times {\rm BR}\Big(\widetilde{\chi}_2^0 \to \widetilde{\chi}_1^0 + \sum_{i=1,\ldots 3} \nu_i\bar{\nu}_i\Big) \\
&+ {\rm BR}\Big(H/A \to \widetilde{\chi}_2^0\widetilde{\chi}_2^0\Big) \times {\rm BR}\Big(\widetilde{\chi}_2^0 \to \widetilde{\chi}_1^0 + \sum_{i=1,\ldots 3} \nu_i\bar{\nu}_i\Big)^2\Bigg] \times {\rm BR}\Big(\widetilde{\chi}_1^0 \to \gamma\widetilde{G}\Big)^2 . \qquad (6)
\end{aligned}$$

In Fig. 1 we display the variation of $\sigma_{\rm eff}$ with $\tan\beta$ for the sets of GMSB parameter space points given in Tab. 7. From the pattern of each curve it is clear that the lower Λ the higher $\sigma_{\rm eff}$. Furthermore, at low $\tan\beta$, $\sigma_{\rm eff}$ is larger than at high $\tan\beta$. This can be understood from the fact that, as $\tan\beta$ grows, the lighter stau ($\tilde{\tau}_1$) becomes the NLSP, with the decay $\widetilde{\chi}_1^0 \to \tilde{\tau}_1^\pm + \tau^\mp$ becoming the dominant one: this explains the sharp fall in $\sigma_{\rm eff}$ at large $\tan\beta$.

The event simulation has been carried out by exploiting the SUSY implementation [15] of the `HERWIG` event generator [16], supplemented by the ISASUSY [10] subroutines (v7.58) interfaced to the `ISAWIG` code [17] for SUSY spectra generation. We list here the series of process numbers used for the MC event generation: i.e.,

```
IPROC = 3320 3360 3375 3630 3815 3826
        3310 3325 3365 3610 3710 3816 3835
        3315 3335 3370 3620 3720 3825 3836
```

for the signal and IPROC = 2200 for the background (corresponding to direct di-photon production $q\bar{q}, gg \to \gamma\gamma$)[8].

As illustrative values for the MC simulation, we have used the three points given in Tab. 8. Notice that they have already been discussed, as they are those appearing in: the fourth row of Tab. 4 (Point 1, which is SPS8 of Ref. [11]), Tab. 5 (Point 2) and Tab. 6 (Point 3).

Table 8: Sets of GMSB parameter points used in the HERWIG simulation and to produce Figs. 2–4.

Point	M [TeV]	Λ [TeV]	N_M	$\tan\beta$	sgn(μ)
1	200	100	1	15	+
2	150	75	1	10	+
3	150	75	1	35	−

The signature we are trying to extract is simply defined as follows, along the lines of the ATLAS/CMS triggers [1, 2].

- Two photons are required: one with $p_T > 40$ GeV and 20 GeV for the other, both within 2.5 in pseudorapidity.
- The two photons are required to have a relative angle less than 175 degrees, in order to enable the mass reconstruction of the two heaviest Higgs bosons decaying into two photons and two LSPs, the latter yielding the missing (transverse) energy.
- No cuts in missing (transverse) energy are enforced at this preliminary stage, nor any restriction on the underlying hadronic activity is imposed.

We then look at:

- $E_{\rm miss}$: the missing (transverse) energy.

This quantity is plotted in Fig. 2(a,b,c), normalised to one. (Hereafter, the labelling a(b)[c] in the figures refers to GMSB set 1(2)[3] as given above in Tab. 8.) As intimated in the Introduction, one may appreciate here the fact that the missing (transverse) energy distribution is much softer for the background, as compared to the signal. A suitable cut on this quantity, which will enhance the

[8]The attentive reader will notice that we have generated in the MC simulations more processes than those used in Fig. 1. This has been done for completeness mainly, as the four channels described in Sect. 3 are indeed those making up most of the visible cross section. Furthermore, all possible decay channels of Higgs bosons and neutralinos are included in the MC simulation, through the ISAWIG input files. Also notice that the (inclusive) rates in Fig. 1 use next-to-leading order normalisation, whereas those in Figs. 2–4 adopt the lowest order one, as default in a MC event generator.

signal-to-background ratio, could be, e.g., $E_{\rm miss} > 20$ GeV. This may penalise signal contributions due to h decays, yet it will have a beneficial impact in extracting those arising from H and A.

Upon enforcing this constraint, in addition to the cuts in 1.–2., we look at two kinematic observables:

- $m_{\gamma\gamma}$: the invariant mass of the photon pair obtained by using their visible momenta;
- $M_{\gamma\gamma}$: the invariant mass of the photon pair obtained after resolving the $E_{\rm miss}$ along the visible photon directions.

These are plotted in Figs. 3(a,b,c) and 4(a,b,c), respectively, normalised to the integrated cross section in picobarns, as given by `HERWIG`. From these plots it is clear the potential of the LHC in detecting di-photon signals of neutral Higgs bosons, as induced by our sample of GMSB model configurations. However, while the direct $h \to \gamma\gamma$ resonance is clearly visible and narrowly centred around M_h in both distributions $m_{\gamma\gamma}$ and $M_{\gamma\gamma}$ (and so it was even prior to the enforcement of the cut in $E_{\rm miss}$), no peak associated to $H/A \to \gamma\gamma + E_{\rm miss}$ decays appears, yet the corresponding events spread over the entire mass range well above the di-photon background. In fact, our mass reconstruction procedure fails because of the many unresolvable sources of missing energy appearing at hadron level, once all decay modes of each unstable particle are allowed, as dictated by the MSSM configuration induced by the underlying GMSB scenario. Here, the exploitation of a more exclusive final state would be helpful to the cause of extracting the H/A resonance. However, we refrain here from pursuing this matter further and simply remark that, even in absence of heavy Higgs mass reconstruction, a clear excess in the di-photon channel above the SM expectations should be established at the LHC after minimal luminosity[9], with some dependence in both the $m_{\gamma\gamma}$ and $M_{\gamma\gamma}$ spectra upon the relevant masses $M_{H/A}$, $M_{\widetilde{\chi}^0}$ and $M_{\tilde{G}}$, whose actual values may be investigated via a comparison of the data to the MC generated distributions.

5 Conclusions

In summary, we have proved that, for some rather natural configurations of the GMSB parameter space consistent with current collider limits, one may be able to extract di-photon signals of all neutral Higgs bosons of the MSSM at the LHC. While, after customary ATLAS/CMS cuts on the two photons, the mass of the lightest state would always be visible in the form of a $\gamma\gamma$ resonance, the presence of the two heaviest states (which are degenerate in mass) can be established, in the form of a clear excess in the total number of $\gamma\gamma + E_{\rm miss}$ events over the corresponding SM predictions, after an additional threshold in missing (transverse) energy is enforced. Thus, after

[9] Recall that higher order QCD corrections to the background are well under control in comparison to the excesses seen in the last two figures, as they are of order 10–20% [18]. Moreover, the contribution to the background due to $qg \to q\gamma$ with the final state light (anti)quark mistagged as a photon, not included here, is also small in comparison.

such a selection, in order to test very specific GMSB model predictions, it suffices to exploit the total event rate. Finally, the study of the kinematics of the entire event sample may allow for the determination of crucial sparticle masses, such as those of the the LSP and NLSP, hence enabling one to strongly constrain the underlying SUSY-breaking mechanism.

Our conclusions are based on a sophisticated MC event simulation but a more rudimentary emulation of detector response (based on Gaussian smearing of the visible tracks). However, our preliminary results are rather encouraging and we do believe that they call for attention on the ATLAS/CMS side, as the $\gamma\gamma$ channel is possibly the most studied one in the context of Higgs boson searches at the upcoming CERN hadron collider.

Acknowledgements

JLD-C is grateful to the CERN Theory division for hospitality and to CONACYT-SNI (Mexico) for financial support. DKG's work is supported by the US DOE contracts DE-FG03-96ER40969 and DE-FG02-01ER41155. He is also grateful to the Southampton Theory Group for hospitality while this paper was being completed. The authors are grateful to Barbara Mele for illuminating discussions during the early stages of the analysis.

References

[1] ATLAS Collaboration, *Technical Proposal*, LHCC/P2 (1994).

[2] CMS Collaboration, *Technical Proposal*, LHCC/P1 (1994).

[3] M. Antonelli and S. Moretti, summary talk given at '13th Convegno sulla Fisica al LEP' (LEPTRE 2001), Rome, Italy, 18-20 April 2001, `hep-ph/0106332`.

[4] K.A. Assamagan *et al.*, 'The Higgs Working Group: Summary Report' of the Workshop 'Physics at TeV Colliders', Les Houches, France, 21 May-1 June 2001, `hep-ph/0203056`; G. Azuelos *et al.*, 'The BSM Working Group: Summary Report', *ibidem*, `hep-ph/0204031`.

[5] For reviews, see:
C. Kolda, talk given at 'SUSY 97', University of Pennsylvania, Philadelphia, May 17-21 1997, preprint IASSNS-HEP-97/90, `hep-ph/9707450`, Nucl. Phys. Proc. Suppl. 62 (1998) 266; G. F. Giudice and R. Rattazzi, Phys. Rep. 322 (1999) 41 and references therein.

[6] H.E. Haber and D. Wyler, Nucl. Phys. B323 (1989) 267.

[7] S. Ambrosanio and B. Mele, Phys. Rev. D55 (1997) 1399.

[8] See: LEP SUSY Working Group web page, `http://www.cern.ch/LEPSUSY/`.

[9] H. Baer and T. Krupovnickas, JHEP 0209 (2002) 038.

[10] F.E. Paige, S.D. Protopopescu, H. Baer and X. Tata, hep-ph/9804321; hep-ph/ 9810440; see also: ftp://penguin.phy.bnl.gov:/pub/isajet/.

[11] B.C. Allanach *et al.*, Eur. Phys. J. C25 (2002) 113.

[12] See, e.g.: D0 Collaboration, Phys. Rev. Lett. 80 (1998) 442.

[13] D. Graudenz, M. Spira and P.M. Zerwas, Nucl. Phys. B453 (1995) 17; Z. Kunszt, S. Moretti and W.J. Stirling, Z. Phys. C74 (1997) 479; M. Spira, Fortsch. Phys. 46 (1998) 203.

[14] See: http://www.desy.de/ ~spira/proglist.html.

[15] S. Moretti, K. Odagiri, P. Richardson, M.H. Seymour and B.R. Webber, JHEP 04 (2002) 028; S. Moretti, preprint CERN-TH/2002-075, IPPP/02/22, DCPT/02/44, May 2002, hep-ph/0205105.

[16] G. Marchesini, B.R. Webber, G. Abbiendi, I.G. Knowles, M.H. Seymour and L. Stanco, Comput. Phys. Commun. 67 (1992) 465; G. Corcella, I.G. Knowles, G. Marchesini, S. Moretti, K. Odagiri, P. Richardson, M.H. Seymour and B.R. Webber, hep-ph/9912396; JHEP 01 (2001) 010; hep-ph/0107071; hep-ph/0201201; hep-ph/0210213.

[17] See: http://www-thphys.physics.ox.ac.uk/users/PeterRichardson/HERWIG/isawig.html.

[18] For a review, see: L. Dixon and M.S. Siu, preprint SLAC-PUB-9654, February 2003, hep-ph/0302233.

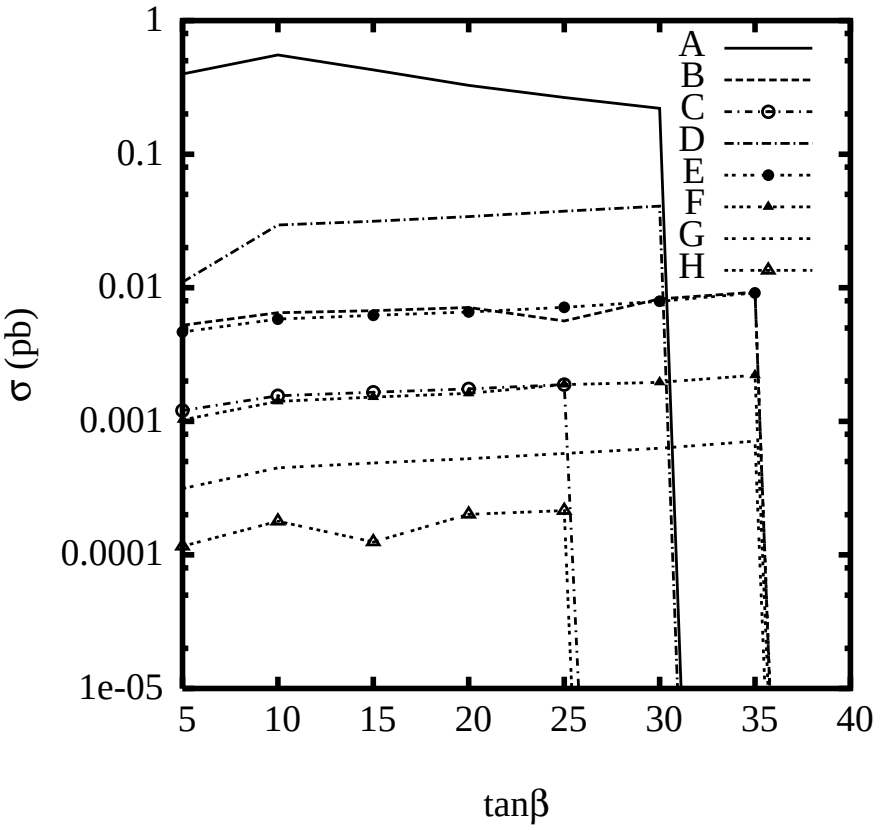

Figure 1: Variation of the effective cross section of eq. (5) with $\tan\beta$ for the representative points in the GMSB parameter space given in Tab. 7.

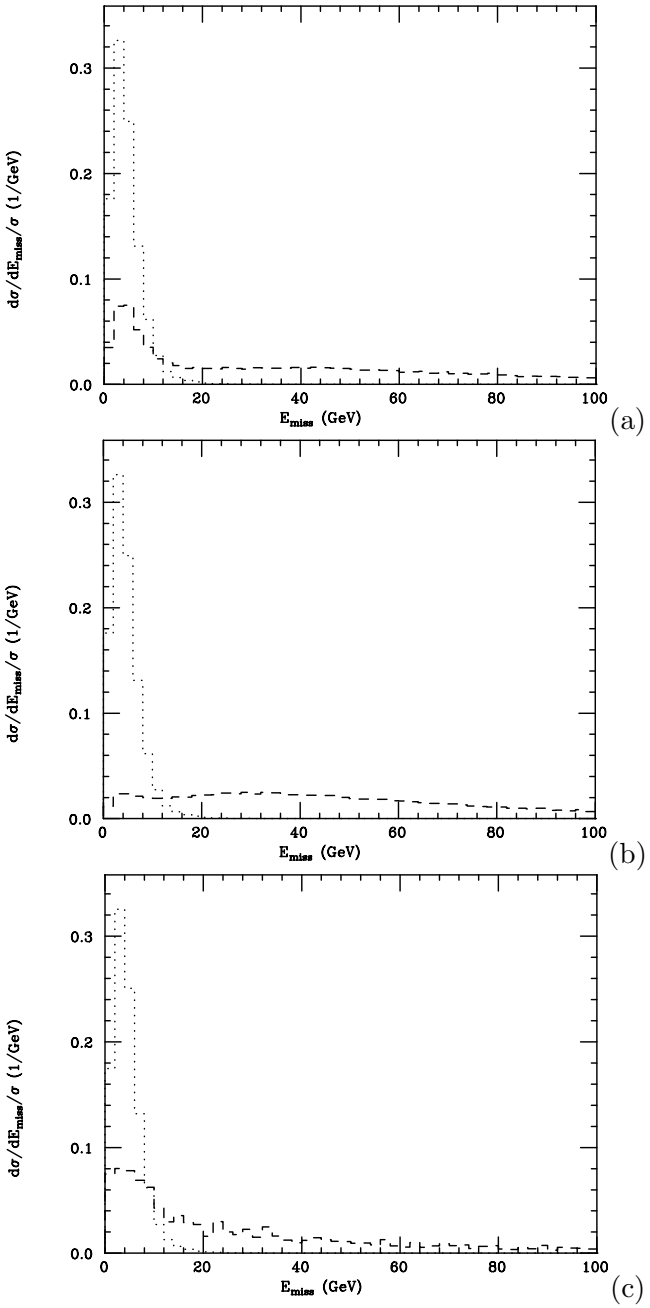

Figure 2: Differential distributions in $E_{\rm miss}$ (as defined in the text) normalised to one, after the cuts 1.–2. described in Sect. 4, as obtained from GMSB set 1 (top), 2 (middle) and 3 (bottom) defined in Tab. 8. The dashed(dotted) line represents the signal(background) rates. Bins are 2 GeV wide.

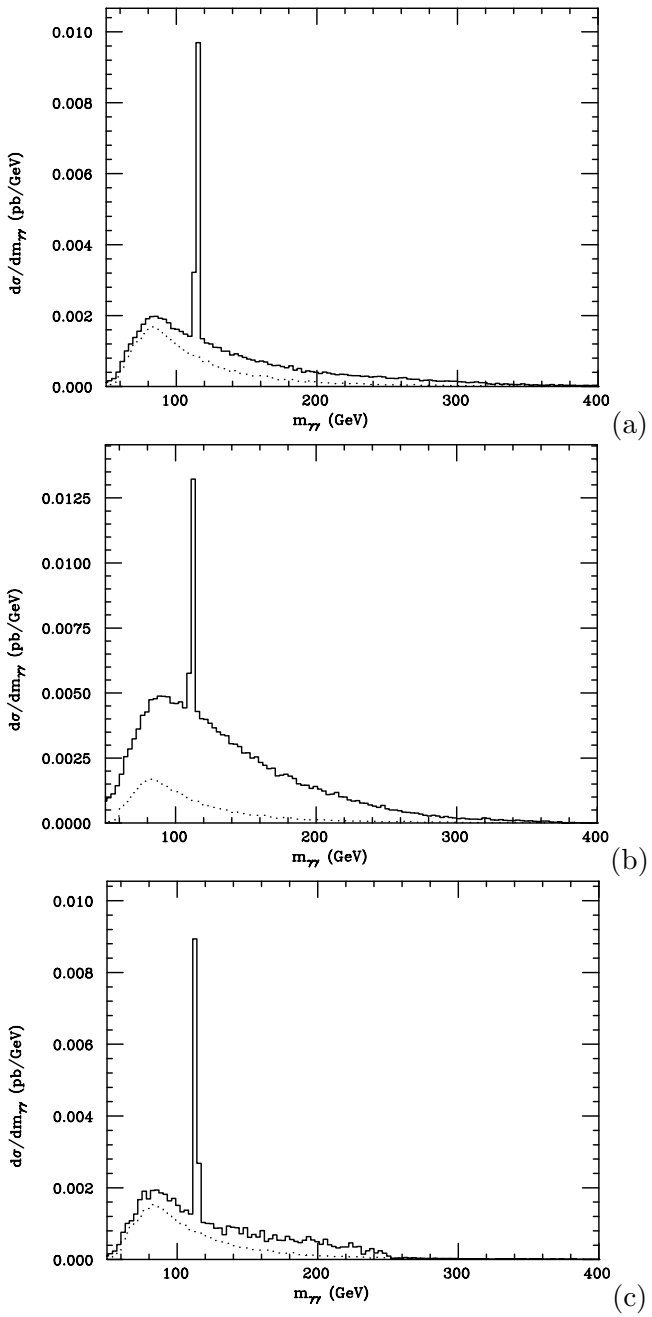

Figure 3: Differential distributions in $m_{\gamma\gamma}$ (as defined in the text) normalised to pb, after the cuts 1.–2. described in Sect. 4 and $E_{\rm miss} > 20$ GeV, as obtained from GMSB set 1 (top), 2 (middle) and 3 (bottom) defined in Tab. 8. The dotted(solid) line represents the background(signal+background) rates. Bins are 3 GeV wide.

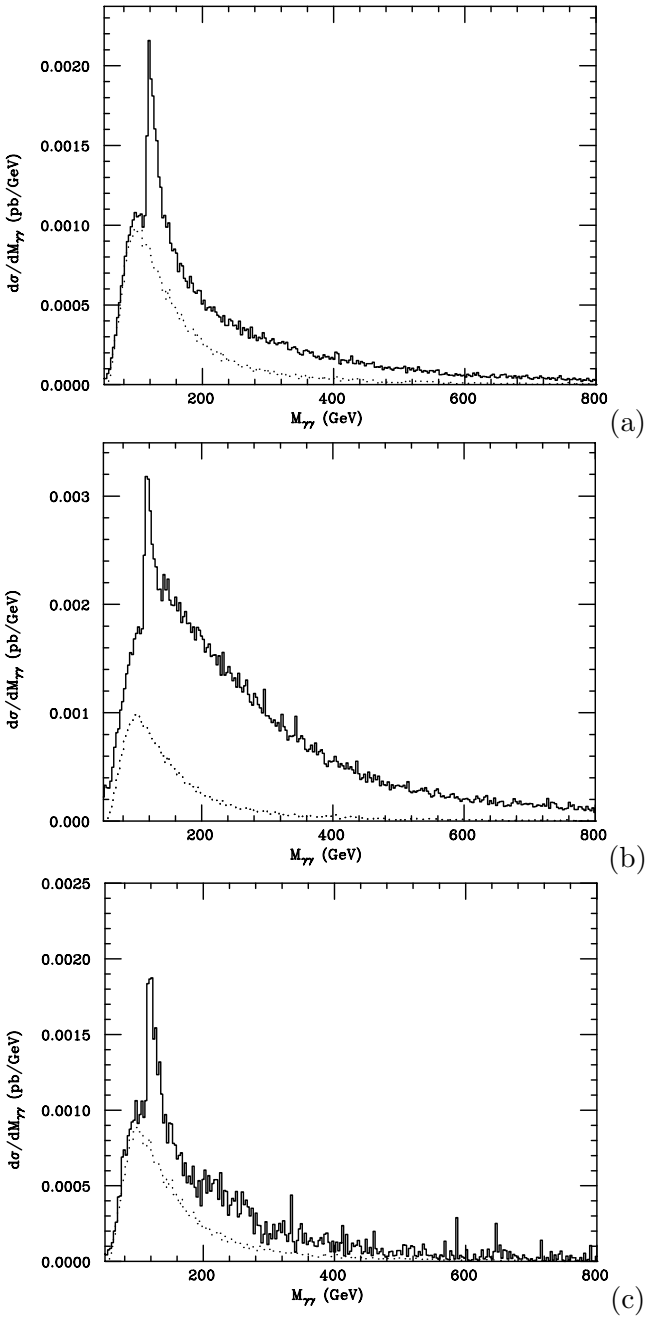

Figure 4: Differential distributions in $M_{\gamma\gamma}$ (as defined in the text) normalised to pb, after the cuts 1.–2. described in Sect. 4 and $E_{\rm miss} > 20$ GeV, as obtained from GMSB set 1 (top), 2 (middle) and 3 (bottom) defined in Tab. 8. The dotted(solid) line represents the background(signal+background) rates. Bins are 3 GeV wide.

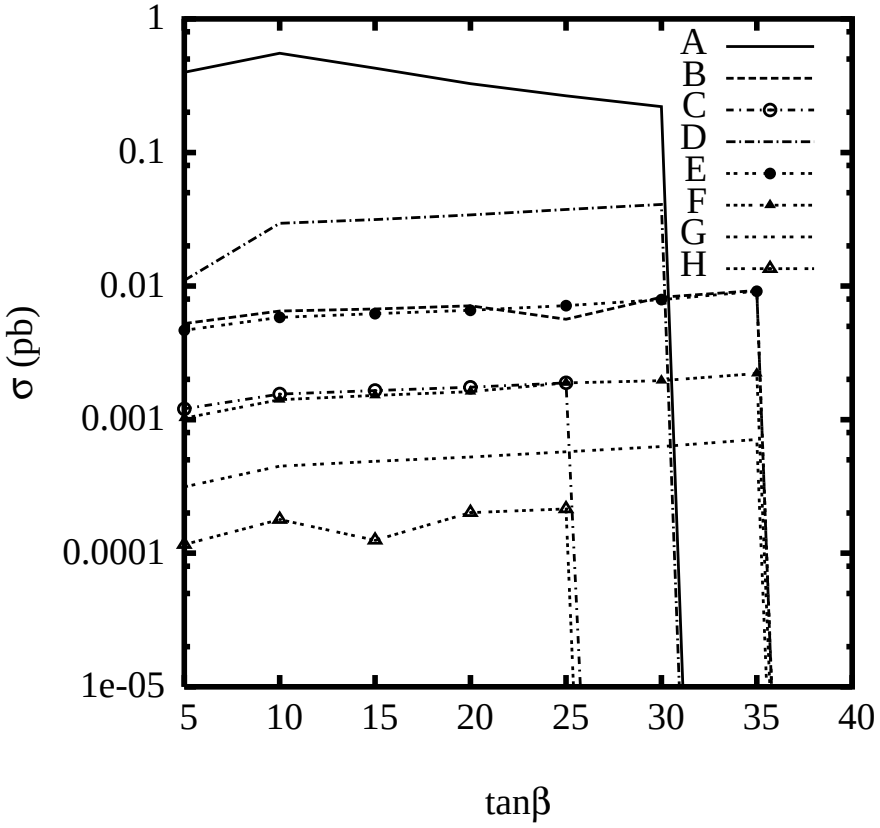
1
0.1
0.01
0.001
0.0001
1e-05
σ (pb)
5
10
15
20
25
30
35
40
tanβ
A
B
C
D
E
F
G
H